THE ASTROPHYSICAL JOURNAL, 975:51 (7pp), 2024 November 1 https://doi.org/10.3847/1538-4357/ad77a4

Effect of Photon Vortex Generated in Extremely Strong Magnetic Fields on Stellar Nucleosynthesis

Tomoyuki Maruyama[1,2], Takehito Hayakawa[3,4], Myung-Ki Cheoun[5], and Toshitaka Kajino[6,7,8]
[1] College of Bioresource Sciences, Nihon University, Fujisawa 252-0880, Japan
[2] Tokyo Metropolitan University, Hachioji, Tokyo 181-8588, Japan
[3] Kansai Institute for Photon Science, National Institutes for Quantum Science and Technology, Kizugawa, Kyoto 619-0215, Japan; hayakawa.takehito@qst.go.jp
[4] Institute of Laser Engineering, Osaka University, Suita, Osaka 565-0871, Japan
[5] Department of Physics and OMEG institute, Soongsil University, Seoul 156-743, Republic of Korea
[6] Beihang University, School of Physics, Peng Huanwu Collaborative Center for Research and Education, International Research Center for Big-Bang Cosmology and Element Genesis, Beijing 100191, People's Republic of China
[7] National Astronomical Observatory of Japan, 2-21-1 Osawa, Mitaka, Tokyo 181-8588, Japan
[8] Graduate School of Science, The University of Tokyo, 7-3-1 Hongo, Bunkyo-ku, Tokyo 113-033, Japan
Received 2024 July 18; revised 2024 September 2; accepted 2024 September 3; published 2024 October 24

Abstract

It is thought that photon vortices are predominantly produced in extremely strong magnetic fields in the Universe. Because the photon vortex may cause significant large angular momentum transfer in interactions with atomic nuclei, stellar nucleosynthesis in such astrophysical environments is affected. In the present study, we calculate the ratios of the photon absorption transition probabilities of photon vortices with Bessel wave to photons described by the plane wave. The result shows enhancement of excitation of states with large total angular momentum by optimization of the divergence angle of the incident photon vortex in momentum space. However, the average cross section for the photon vortex turns out to be identical with that for the plane wave. Therefore, even when Bessel photons are predominantly produced in astrophysical environments, the isotopic abundances of the synthesized elements are not changed.

Unified Astronomy Thesaurus concepts: R-process (1324); P-process (1195); Nuclear reaction cross sections (2087)

1. Introduction

Since the proposal of optical vortices by L. Allen et al. (1992), the field of optical vortices has made significant progress in fundamental science (U. D. Jentschura & V. G. Serbo 2011; E. Hemsing et al. 2013; V. Petrillo et al. 2016; J. A. Sherwin 2017; A. A. Peshkov et al. 2018; T. Maruyama et al. 2019) and in various applications (Y. Shen et al. 2019). Furthermore, L. Allen et al. (1992) have also proposed photon vortices in the quantum level. One of the remarkable features of the photon vortex is that it is the eigenstate of the z-component of the total angular momentum (zTAM) when the photon propagates along the z-axis. This plays an important role in interactions with quantum objects such as molecules (M. Babiker et al. 2002; A. Alexandrescu et al. 2006), atoms (A. Picón et al. 2010; A. Afanasev et al. 2013), atomic nuclei (A. Afanasev et al. 2018; Z. W. Lu et al. 2023; Y. Xu et al. 2024), and nucleons (A. Afanasev & C. E. Carlson 2022) because quantum effects can arise from significant angular momentum transfer. The wave functions known for photon vortices are those based upon Laguerre–Gaussian wave (T. Maruyama et al. 2019) and Bessel wave (R. Jáuregui & S. Hacyan 2005; T. Maruyama et al. 2022; T. Maruyama 2023) have been known. The generation of the photon vortex was experimentally examined using quantum entanglement (A. Mair et al. 2001; J. Leach et al. 2002). Furthermore, the selective excitation of an atom with optical vortices was demonstrated (C. T. Schmiegelow et al. 2016; R. Lange et al. 2022).

The potential natural origin of optical vortices in the Universe has also been theoretically explored (M. Harwit 2003; G. Anzolin et al. 2008; G. C. G. Berkhout & M. W. Beijersbergen 2008; N. M. Elias 2008; F. Tamburini et al. 2011; Y. A. Portnov 2018; T. Maruyama et al. 2022). It has been predicted that the optical vortex is generated by strong gravity fields around rotating black holes (F. Tamburini et al. 2011), and the optical vortex of the Laguerre–Gaussian mode with frequency of approximately 200 GHz from the M87 black hole was measured (F. Tamburini et al. 2020). Although the optical vortex generated in black holes is in the Laguerre–Gaussian mode, photon vortices of the Bessel wave are also considered to be generated in the Universe. Synchrotron radiations from spiral-moving electrons under strong uniform magnetic fields is expected to be the source of Bessel photons (M. Katoh et al. 2017; O. V. Bogdanov et al. 2018, 2019; T. Maruyama et al. 2022; T. Maruyama 2023). The generation of photon vortices of the Bessel wave in an energy region of MeV through synchrotron radiation in an extremely strong uniform magnetic field ranging from 10^8 to 10^{10} T has been calculated (T. Maruyama et al. 2022). Such conditions could exist in celestial systems such as magnetized neutron stars (S. Mereghetti 2008), jets, and accretion disks around black holes (J. C. McKinney et al. 2013), which are considered to be central engines of X-ray pulses and γ-ray bursts.

The photons in the MeV energy region have important roles in the synthesis of elements through interaction between photons and atomic nuclei. The differences in nuclear reactions between photon vortices of the Bessel wave and plane wave photons have been discussed (A. Afanasev et al. 2018; Z. W. Lu et al. 2023; Y. Xu et al. 2024). A. Afanasev et al. (2018) calculated photodisintegration reactions on a deuteron with a photon vortex. It was shown that the cross section of a high-spin mode is a function of the impact parameter b, which is the minimum distance between a nucleus and a photon vortex. Y. Taira et al. (2017) have suggested the possibility that giant dipole resonances (GDRs) should be forbidden because of the selection rule of angular momentum. It was also suggested that when photon vortices are predominantly generated in supernova explosions, the stellar nucleosynthesis by nuclear photoreactions is affected (Y. Taira et al. 2017). The neutron-deficient stable isotopes, the so-called "p nuclei," are synthesized by subsequent nuclear photoreactions such as (γ, n) and (γ, α) reactions in extremely high-temperature environments such as supernova explosions (S. E. Woosley & W. M. Howard 1978; T. Hayakawa et al. 2004). When photon vortices are predominantly produced in such conditions, the produced abundances of the p nuclei should decrease because nuclear photoreactions though GDR with the photon vortex are suppressed. The (γ, n) reactions contribute to other nucleosyntheses such as the r-process. It was also suggested that nucleosynthesis flows of the r-process in strong magnetic fields such as the magnetohydrodynamical supernovae (S. Nishimura 2006) and jets from black holes (K. Nakamura et al. 2015) are affected by the change of (γ, n) reaction rates (T. Maruyama et al. 2022).

In a recent study (Z. W. Lu et al. 2023), giant resonance excitation by absorption by photon vortices was studied. The authors show that when a target nucleus exists on a photon vortex propagation axis, excitation of low multipole giant resonances is forbidden due to the selection rule of angular momentum. It is also shown that enhancement of giant quadrupole and octupole resonances ocurrs in the cases of small b value. Furthermore, it was presented that the cross sections of photon-induced reactions with photon vortex with zTAM of 2 at specific angles are different from those with zTAM of 1 (Y. Xu et al. 2024). In addition, 138 nuclei to be affected by nuclear photoreactions with photon vortices in the Universe are systematically studied (Y. Xu et al. 2024), where the difference between the cross sections of photon vortices with zTAM of 1 and 2 are calculated. These studies suggest the possibility that the isotopic abundances of elements synthesized in an extremely strong magnetic field are different from those without such fields and that the galactic chemical evolution of the elements should be modified by considering the photon vortex interactions. The question that we should answer is the difference of the total photon absorption reaction cross sections between the photon vortices and photons described by the plane wave.

In the present study, we first confirm the cross section ratio of the photon vortex to the plane wave photon, which has been studied in previous studies (Z. W. Lu et al. 2023; Y. Xu et al. 2024). An excitation state has a total angular momentum J and z-projection M when the incident photon with zTAM of K travels along the z-axis. In most cases, the ratio for excitation of states with $J = K$ is the highest. We also show that the ratio for states with $J > K$ becomes higher than that for $J = K$ when the divergence angle of the incident photon vortex is optimized. We finally show that the total cross section for the photon vortex is identical to that for the plane wave photon. This means that the stellar nucleosynthesis is not affected by photon vortex generation in the Universe.

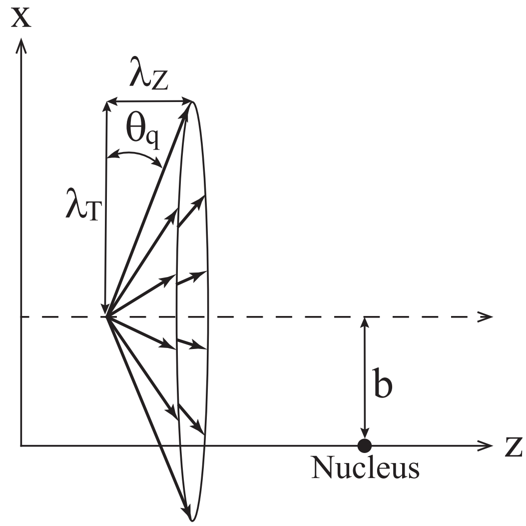

Figure 1. Schematic view of the photon vortex and the nucleus in the coordinate space.

2. Calculation

2.1. Ratio of Photon Absorption Transition Probability between the Bessel Wave and the Plane Wave

In the present study, we consider the interaction between a photon vortex (twisted photon) described by the Bessel wave and the ground state with $J^{\pi} = 0^{+}$ of an atomic nucleus. We use the natural unit. As presented previously, the Bessel wave is the eigenstate of zTAM when the photon propagates along the z-axis and can bring a large intrinsic angular momentum of zTAM $\geqslant 1$. The Bessel wave function at fixed zTAN of K has two orthogonal states: the transverse magnetic and the transverse electric states (R. Jáuregui & S. Hacyan 2005; T. Maruyama et al. 2022), and they are the linear combination of the two helicity states of $h \pm 1$ (O. V. Bogdanov et al. 2018). In the present calculation, we use the helicity states propagating along the z-direction whose wave functions are written as

$$A_K^h(\boldsymbol{r}) = e^{iq_z z}\left[\frac{i(e_q + hq_z)}{2e_q}\tilde{J}_{K-1}\boldsymbol{e}_{+1} - \frac{i(e_q - hq_z)}{2e_q}\tilde{J}_{K+1}\boldsymbol{e}_{-1} + \frac{hq_T}{\sqrt{2}\,e_q}\tilde{J}_K\boldsymbol{e}_0\right], \tag{1}$$

$$\tilde{J}_M(q_T\boldsymbol{r}_T) = J_M(q_T r_T)e^{iM\phi}, \tag{2}$$

with $\boldsymbol{e}_0 = (0, 0, 1)$ and $\boldsymbol{e}_h = -h(1, ih, 0)/\sqrt{2}$ when $h = \pm 1$, where J_M is the Mth Bessel function, e_q is the photon energy, and q_T and q_z are the longitudinal and transverse momenta of the photon, respectively, with a relationship of $q_T = \sqrt{{e_q}^2 - {q_z}^2}$. We define the sizes of the photon vortex in the longitudinal and transverse direction as $\lambda_z \equiv 1/q_z$ and $\lambda_T \equiv 1/q_T$, respectively, to discuss the correlation between the photon size and the minimum distance between the photon and the nucleus (Figure 1). θ_q is the polar angle defined as $\theta_q \equiv \arctan(\lambda_z/\lambda_T) = \arctan(p_T/p_z)$, indicating the divergence angle of the Bessel photon in the momentum space.

The Bessel wave can be described by a superposition of the plane wave $e^{i\boldsymbol{p}\cdot\boldsymbol{r}}\boldsymbol{e}(\boldsymbol{p}, h)$, which is explained later. To calculate the photon–-nucleus interaction, we expand the Bessel wave to the plane wave by Fourier transformation. The Bessel wave can be presented as

$$\boldsymbol{A}_K^h(\boldsymbol{r}) = \int \frac{d^3p}{(2\pi)^3} A_K^h(\boldsymbol{p}) e^{i\mathbf{p}\cdot\mathbf{r}} \boldsymbol{e}(\boldsymbol{p}, h), \tag{3}$$

$$A_K^h(\boldsymbol{p}) = \frac{(2\pi)^2}{q_T} \delta(p_z - q_z)\delta(p_T - q_T)(-i)^K e^{iK\phi_p}, \tag{4}$$

where the $\boldsymbol{e}(\boldsymbol{p}, h)$ is the polarized vector of the photon with a momentum $\boldsymbol{p}$ and a helicity h:

$$\boldsymbol{e}(\boldsymbol{p}, h) = \frac{(1 + h\cos\theta_p)}{2} e^{-i\phi_p} \boldsymbol{e}_{+1} + \frac{(1 - h\cos\theta_p)}{2} e^{i\phi_p} \boldsymbol{e}_{-1} - \frac{h\sin\theta_p}{\sqrt{2}} \boldsymbol{e}_0, \tag{5}$$

where ϕ_p is the azimuthal angle and θ_p is the polar angle. The helicity of each polarized vector is defined as the spin projection along the propagation axis of the momentum $\boldsymbol{p}$. In the spherical multipole expansion, the plane waves can be expanded (T. de Forest & J. D. Walceck 1966) as

$$\boldsymbol{e}(\boldsymbol{p}, h) e^{i\boldsymbol{p}\cdot\boldsymbol{r}} = \sum_{JM,\kappa} \sqrt{2\pi(2J+1)} (i)^J \mathcal{D}^J_{M,h}(\phi_p, \theta_p, 0) \times [h\boldsymbol{T}^{\mathrm{mag}}_{Jh} + \boldsymbol{T}^{el}_{Jh}], \tag{6}$$

where $\mathcal{D}^J_{M,h}(\phi_p, \theta_p, 0) = \exp(-iM\phi_p) d_{Mh}(\theta_p)$ is the Wigner D-function with $d_{M,h}$ being the Wigner d-matrix and $\boldsymbol{T}^{\mathrm{mag}}_{Jh}$ and $\boldsymbol{T}^{el}_{Jh}$ are components indicating excitation of the parity states with $(-)^J$ and with $(-)^{J+1}$, respectively. Using the parity index κ, these two components are described as $\boldsymbol{T}^{\kappa}_{JM} = h\boldsymbol{T}^{\mathrm{mag}}_{JM}$ for $\kappa = (-)^J$ and $\boldsymbol{T}^{\kappa}_{JM} = \boldsymbol{T}^{el}_{JM}$ for $\kappa = (-)^{J+1}$.

Because the Bessel wave has a propagation axis, we should consider that the minimum distance between a target nucleus and the photon vortex for general cases. We introduce the shift vector $\boldsymbol{b}$, whose absolute value $b \equiv |\boldsymbol{b}|$ corresponds to the impact parameter (Figure 1). We rewrite the Bessel wave with the shift vector as

$$\begin{aligned}\boldsymbol{A}_K^h(\boldsymbol{r} - \boldsymbol{b}) &= \int \frac{d^3p}{(2\pi)^3} A_K^h(\boldsymbol{p}) \boldsymbol{e}(\boldsymbol{p}, h) e^{i\boldsymbol{p}\cdot(\boldsymbol{r}-\boldsymbol{b})} \\ &= \int \frac{d^3p}{(2\pi)^3} e^{-i\boldsymbol{p}\cdot\boldsymbol{b}} \frac{(2\pi)^2}{q_T} \delta(p_z - q_z)\delta(p_T - q_T)(-i)^K e^{iK\phi_p} \\ &\quad \times \sum_{J,M,\kappa} \sqrt{2\pi(2J+1)} (i)^J e^{-iM\phi_p} d^J_{M,h}(\theta_p)(\hat{p}) \boldsymbol{T}^{\kappa}_{JM}.\end{aligned} \tag{7}$$

We define the transition operators as

$$\hat{T}^{el(\mathrm{mag})}_{JM} \equiv \int d^3r \hat{\boldsymbol{J}}_{\mathrm{nuc}}(\boldsymbol{r}) \cdot \boldsymbol{T}^{el(\mathrm{mag})}_{JM}, \tag{8}$$

where $\hat{\boldsymbol{J}}_{\mathrm{nuc}}$ is the nucleus current operator. Using the Wigner–Eckart theorem, the transition amplitude for the operator $\hat{T}^{\kappa}_{JM}$ can be calculated as

$$\begin{aligned}\langle J, M, \kappa | \hat{T}^{\kappa}_{JM} | 0, 0, + \rangle &= \langle 00JM|JM \rangle \langle J, \kappa \| T^{\kappa}_J \| 0, + \rangle \\ &= \frac{1}{\sqrt{2J+1}} \langle J, \kappa \| T^{\kappa}_J \| 0, + \rangle\end{aligned} \tag{9}$$

where $\|T^{\kappa}_J\|$ is the reduced matrix element, which is independent of M.

At a fixed impact parameter b, we obtain the transition probability for the Bessel wave photon with a zTAM of K and a helicity of h from the ground state with $J^{\pi} = 0^+$ to an excited state with a total angular momentum of J, a z-direction projection of the total angular momentum of M, and a party of κ as

$$\begin{aligned}P^{Kh}_{JM\kappa}(b) &= \left| \left\langle J, M, \kappa \left| \int d^3r \hat{\boldsymbol{J}}_{\mathrm{nuc}}(\boldsymbol{r}) \cdot \boldsymbol{A}^h_K(\boldsymbol{r} - \boldsymbol{b}) \right| 0, 0, + \right\rangle \right|^2 \\ &= 2\pi\, |d^J_{M,h}(\theta_q)|^2 [J_{M-K}(q_T b)]^2 \|T^{\kappa}_J\|^2.\end{aligned} \tag{10}$$

The transition probability depends on θ_q and q_T.

We here obtain the ratio of the transition probabilities of the photon vortex to the plane wave photon. When the initial photon is the plane wave with the momentum $\boldsymbol{q} = (0, 0, e_q)$, its wave function can be written as

$$e^{ie_q z} \boldsymbol{e}(\boldsymbol{q}, h) = \sum_{J=1}^{\infty} \sqrt{2\pi(2J+1)} (i)^J \sum_{\kappa} \boldsymbol{T}^{\kappa}_{Jh}, \tag{11}$$

and the transition probability is given by

$$\begin{aligned}\mathcal{P}^{(0)}_{J\kappa} &= \left| \left\langle J, h, \kappa \left| \int d^3r (\hat{J}_{\mathrm{nuc}}(r) \cdot e(q, h)) e^{\mathrm{i}e_q z} \right| 0, 0, + \right\rangle \right|^2 \\ &= 2\pi\, \|T^{\kappa}_{\mathrm{Jh}}\|^2.\end{aligned} \tag{12}$$

For the initial state of $J^{\pi} = 0$, the transition probability does not depend on the helicity h.

We obtain the ratio of the transition probabilities between the Bessel wave of Equation (10) and the plane wave of Equation (12) for the incident photon at an impact parameter b as

$$\frac{P^{Kh}_{JM\kappa}(b)}{\mathcal{P}^{(0)}_{J\kappa}} = |d^J_{M,h}(\theta_q)|^2 [J_{M-K}(q_T b)]^2. \tag{13}$$

The photon vortex absorption excites the ground state to a state with M in a range of $-J \leqslant M \leqslant J$, whereas the plane wave photon absorption excites only to two states with $M = \pm 1$. We sum it over M and obtain the transition ratio at the impact parameter b as

$$R_K(b) = \sum_{M=-J}^{J} \frac{P^{Kh}_{JM\kappa}(b)}{\mathcal{P}^{(0)}_{J\kappa}} = \sum_{M=-J}^{J} |d^J_{M,h}(\theta_q)|^2 [J_{M-K}(q_T b)]^2. \tag{14}$$

This ratio is consistent with the previous results (Z. W. Lu et al. 2023; Y. Xu et al. 2024). Using $\lambda_T \equiv 1/q_T$, we can plot $R_K(b)$ as a function of a dimensionless value of b/λ_T (Figures 2 and 3). The previous studies (Z. W. Lu et al. 2023; Y. Xu et al. 2024) indicated that the probability of the photon vortex absorption became larger near the nucleus. For example, the enhancement can be observed in an area within 50 fm for the assumed condition (Y. Xu et al. 2024). In these studies, the relatively large divergence angles of $\theta_q = 10°–30°$ were assumed for the initial photon vortices. However, as θ_q decreases λ_T increases (Figure 1) and the effectively photon absorption region near the nucleus expands. Equation (14) shows that the ratio depends only on the d-matrix and Bessel function $J_M(b)$, and $J_M(b)$ has nonzero value at $b = 0$ when only $M = 0$, whereas $J_M(b)$ for $M \geqslant 1$ vanishes at $b = 0$. Therefore,

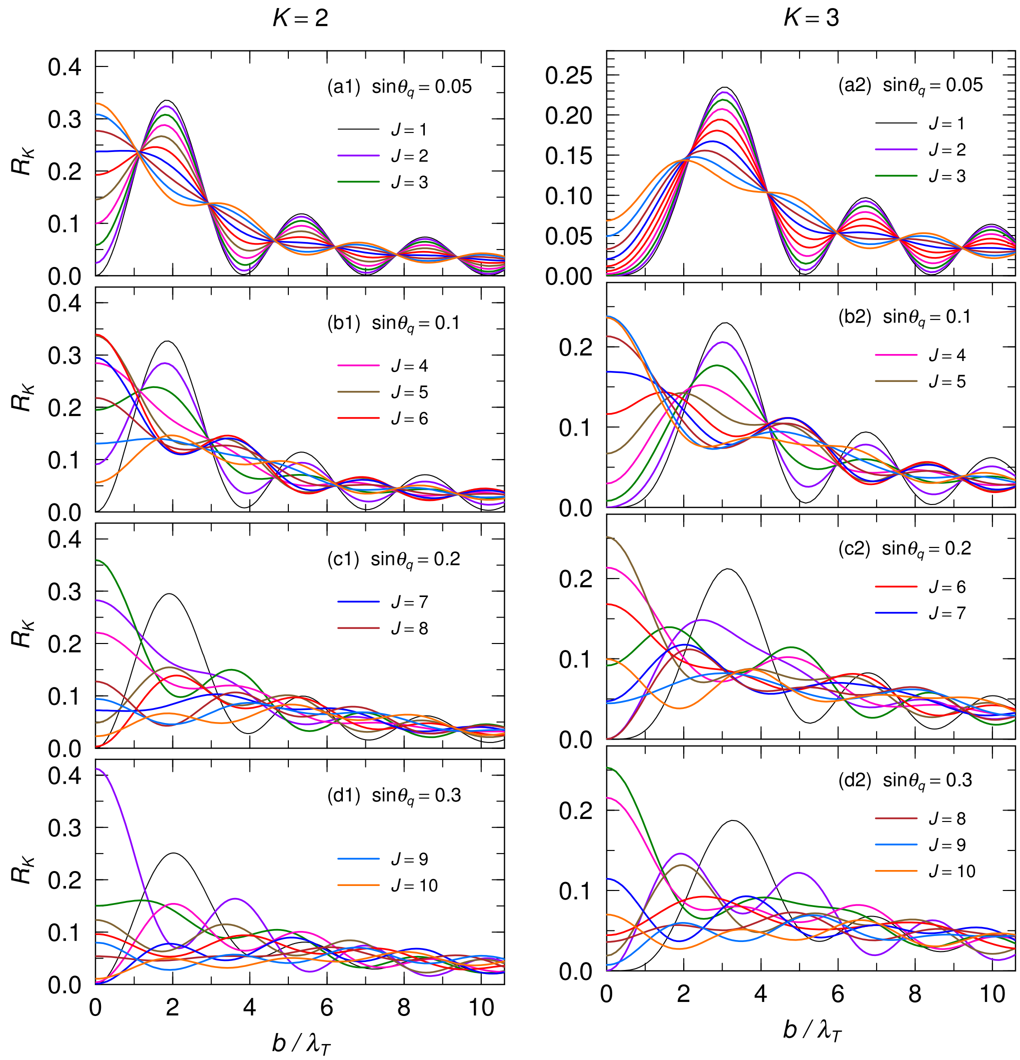

Figure 2. Ratio of the photon absorption from a ground state of $J^{\pi} = 0^{+}$ in a nucleus between Bessel wave and plane wave as a function of b/λ_T for $K = 2$ and 3. K means the zTAM of the incident photon vortex when it propagates along z-axis, and J shows the total angular momentum of the excited state. θ_q is the divergence angle of the incident photon vortex in the momentum space.

the enhancement of the ratio at $b = 0$ comes only from the contribution of the excitation of the state with $M = K$ for $J \geqslant M$. Figure 2(b1) shows that when a photon vortex with $K = 2$ and $\sin\theta_q = 0.1$ interacts with a nucleus, R_K for the excited states with $J = 3$ and 4 is higher than that for $J = 2$. However, for larger $\sin\theta_q$, the enhancement of R_K with $J > K$ becomes weak, and in the case of $\sin\theta_q = 0.3$, R_K with $J = K$ becomes the highest. This trend is also observed for incident photon vortices with $K \geqslant 3$. These results show that the optimization of θ_q is important for the observation of the higher-order multipole excitation as well as high-spin excited states. When we choose a relatively small angle for θ_q, it gives the advantage of a wider size of λ_T, which may be useful for experiments.

2.2. Possible γ-Ray Sources

One of the expected generation methods of γ-ray vortices is Compton scattering on high-energy electrons of optical vortex (U. D. Jentschura & V. G. Serbo 2011; S. Stock et al. 2015; V. Petrillo et al. 2016; J. A. Sherwin 2017). When a optical vortex is generated from laser with an optical device, it is expected that photon vortices with the Laguerre–Gaussian wave (T. Maruyama et al. 2019) is generated through this Compton scattering. If Bessel wave photons are used for Compton scattering, Bessel γ-rays are generated. Synchrotron radiations from spiral-moving electrons under strong magnetic fields is expected to be one of the sources of Bessel photons (M. Katoh et al. 2017; O. V. Bogdanov et al. 2018, 2019; T. Maruyama et al. 2022; T. Maruyama 2023). One of the other candidates is nonlinear Compton scattering in an electron with a circularly polarized high-flux laser (Y. Taira et al. 2017; X. X. Zhu et al. 2018; Y.-Y. Chen et al. 2018; M. Ababekri et al. 2024), and photons described by the Bessel wave (R. Jáuregui & S. Hacyan 2005; T. Maruyama 2023) are generated. When these high-energy photon vortices are provided, it is possible to measure large angular momentum transfer effects in the interaction with nucleus and nucleons such as higher-order multipole resonances.

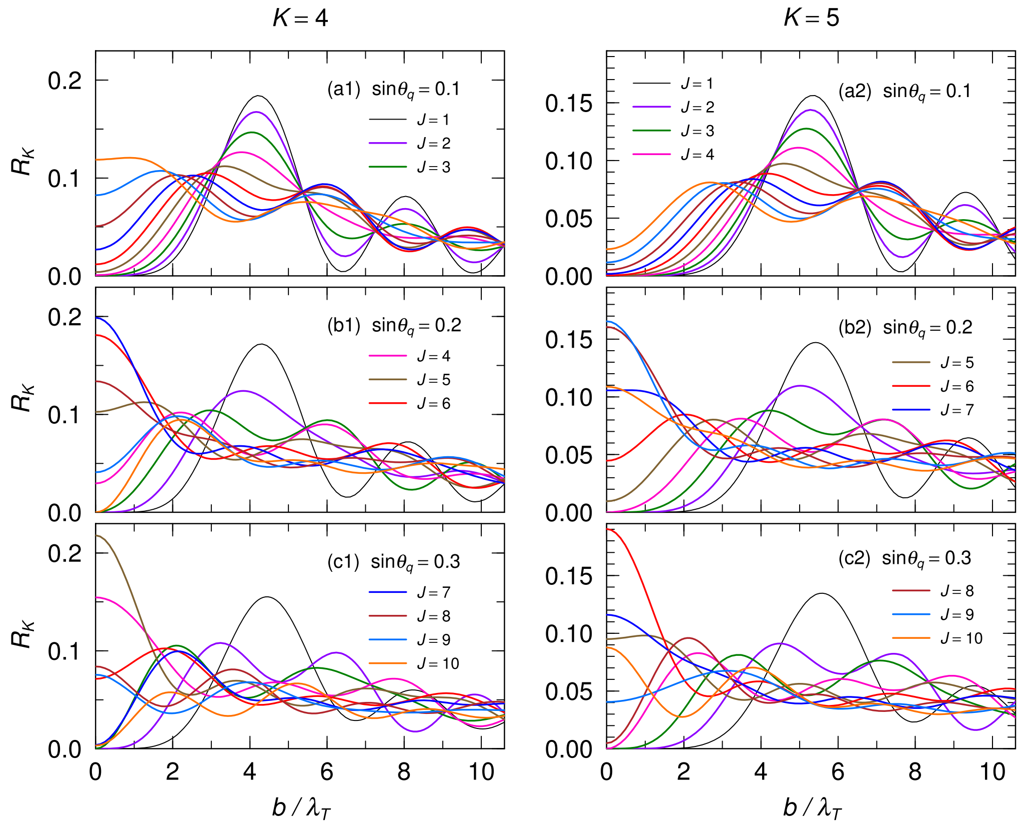

Figure 3. Ratio of the photon absorption from a ground state of $J^{\pi}=0^{+}$ in a nucleus between Bessel wave and plane wave as a function of b/λ_T for $K=4$ and 5.

2.3. Total Transition Probability

The previous studies (Y. Taira et al. 2017; T. Maruyama et al. 2022; Y. Xu et al. 2024) suggested that when the cross sections of nuclear photoreactions with photon vortices are different from those with photons described by the plane waves, the stellar nucleosynthesis is affected. Furthermore, the recent studies for photon vortex generation in the Universe also suggest photon vortices are predominantly produced with specific conditions such as strongly magnetized neutron stars (T. Maruyama et al. 2022). Although we have calculated the transition probabilities for the Bessel wave and plane wave from the ground state with $J^{\pi}=0^{+}$, we here calculate the transition probabilities for various initial states. We extend the transition amplitude for the operator $\hat{T}^{\kappa}_{JM}$ expressed by Equation (10) for any initial spin and parity state as

$$\begin{aligned}\langle J_f,\, M_f,\, \kappa_f|\hat{T}^{\kappa}_{JM}|J_i,\, M_i,\, \kappa_i\rangle &= \frac{1}{\sqrt{2J_f+1}}\\ &\times \langle J_i M_i J M|J_f M_f\rangle \quad \langle J_f,\, \kappa_f\|T^{\kappa}_{J}\|J_i,\, \kappa_i\rangle\\ &= \frac{(-)^{J-J_f+M_i}}{\sqrt{2J+1}}\delta_{\kappa\kappa_i\kappa_f,+1}\langle J_f M_f J_i - M_i|JM\rangle\\ &\langle J_f,\, \kappa_f\|T^{\kappa}_{J}\|J_i,\, \kappa_i\rangle. \end{aligned}\tag{15}$$

Using this equation, we obtain the transition probability for an initial state with J_i, M_i, and κ_i to another state with J_f, M_f, and κ_f for the Bessel wave as

$$\begin{aligned}&P^{Kh}_{JM\kappa}(J_f,\, \kappa_f,\, J_i,\, \kappa_i;\, b)\\ &= \frac{1}{(2J_i+1)}\sum_{M_i,M_f}\Big|\,\langle J_f,\, M_f,\, \kappa_f|\int d^3r\hat{\boldsymbol{J}}_{\rm nuc}(\boldsymbol{r})\cdot \boldsymbol{A}^{h}_{K}\\ &\times(\boldsymbol{r}-\boldsymbol{b})|J_i,\, M_i,\, \kappa_i\rangle|^2\\ &= \frac{2\pi}{(2J_i+1)}\delta_{\kappa\kappa_i\kappa_f,+1}\,|d^{J}_{M,h}(\theta_q)|^2\,[J_{M-K}(q_T b)]^2\,\|T^{\kappa}_{J}\|^2. \end{aligned}\tag{16}$$

We also modify the average transition probability for the plane wave of Equation (12) for any initial spin and parity states as

$$\begin{aligned}\mathcal{P}^{(0)}_{J\kappa} &= \frac{1}{(2J_i+1)}\sum_{M_i,M_f}|\langle J_f,\, M_f,\, \kappa_f|\\ &\times\int d^3r(\hat{J}_{\rm nuc}(r)\cdot e(q,\, h))e^{{\rm i}e_q z}\,|J_i,\, M_i,\, \kappa_i\rangle|^2\\ &= \frac{2\pi}{(2J_i+1)}\delta_{\kappa\kappa_i\kappa_f,+1}\,\|T^{\kappa}_{\rm Jh}\|^2. \end{aligned}\tag{17}$$

The previous studies (Z. W. Lu et al. 2023; Y. Xu et al. 2024) calculated the cross sections with photon vortices as a function of b or in a limited region close to a target nucleus for b. The control of the impact parameter is possible in the laboratory. However, in the Universe, photon vortices interact with nuclei with various minimum distances, and there is no limitation for the impact parameter b. Therefore, we explore the average transition probability integrated by the impact parameter b. Because the Bessel wave has infinite size in the xy-plane when the Bessel wave propagates along the z-axis, we integrate the transition probability for the impact parameter b from 0 to infinity to obtain exactly the total transition probability. After the integration, we obtain the average transition probability by dividing it by the area of the system S_T. Using Equation (16), the average transition probability is written as

$$\mathcal{P}^{Kh}_{JM\kappa} = \frac{1}{S_T}\sum_{M_i,M_f}\int d\boldsymbol{b}\,\Big|\int d^3r\,\langle J_f,\,M_f,\,\kappa_f|\hat{\boldsymbol{J}}_{\rm nuc}(\boldsymbol{r})\cdot\boldsymbol{A}^h_K \times(\boldsymbol{r}-\boldsymbol{b})|J_i,\,M_i,\,\kappa_i\rangle\Big|^2 = \frac{(2\pi)^6}{(2\pi)^6 S_T}\frac{\delta_{\kappa\kappa_i\kappa_f,+1}}{(2J_i+1)}\int d^3p_1\frac{(2\pi)^2[\delta(p_{1T}-q_T)]^2}{q_T^2}\delta \times(p_{1z}-q_z)|d^J_{M,h}(\theta_{p1})|^2\|T^\kappa_J\|^2. \quad (18)$$

The S_T can be taken to be $S_T = (2\pi)^2\delta(p_{1T} - q_T)/q_T$, and the above equation is rewritten as

$$\mathcal{P}^{Kh}_{JM\kappa} = \frac{2\pi}{(2J_i+1)}\delta_{\kappa\kappa_i\kappa_f,+1}\,|d^J_{M,h}(\theta_q)|^2\|T^\kappa_J\|^2. \quad (19)$$

By summing the above quantity over M, we obtain

$$\mathcal{P}^K_{J\kappa} = \sum_M \mathcal{P}^{Kh}_{JM\kappa} = \frac{2\pi}{(2J_i+1)}\delta_{\kappa\kappa_i\kappa_f,+1}\|T^\kappa_J\|^2. \quad (20)$$

This equation is identical with Equation (17) for the plane wave photon. Therefore, the average cross sections for the Bessel photon and plane wave photon are the same.

In general, nuclei in stellar environments are excited under thermal equilibrium. Thus, to obtain the reaction rate with photon vortices for stellar nucleosynthesis, one should calculate the reaction rate in excited states under thermal equilibrium (H. Utsunomiya et al. 2006). Although the energy distribution of Bessel photons depends on astrophysical environments, it is expected to follow thermal distribution in most cases. The present result shows that the two transition probabilities for the Bessel wave and plane wave from an excited state or the ground state to another excited state are identical. The reduced matrix element does not depend on the wave function of the incident photon in spherical multipole expansion, and thus, the reaction rate on excited states for Bessel photons can be also calculated using the Brink–Axel hypothesis (M. Markova et al. 2021; K. Sieja 2023). This result indicates that even if Bessel photons are predominantly produced in astrophysical environments, the reaction rates in the stellar nucleosynthesis are not changed. Note that when photon vortices of the Laguerre–Gaussian wave are produced in rotating black holes, the isotopic abundances of the r-process around the black holes may be changed, but it is beyond the scope of this study.

3. Summary

In summary, the ratios of the photon absorption cross sections of the Bessel wave with zTAM of K to the plane wave on a nucleus show that the enhancement of excitation to states with the z-projection of the total angular momentum of $M = K$ could be observed in an area of $b/\lambda_T < 1$, where b is the impact parameter and λ_T is the transverse size of the Bessel photon. This is consistent with the previous results (Z. W. Lu et al. 2023; Y. Xu et al. 2024). Furthermore, it is shown that the ratios for excitation to states with $J > K$ and $M = K$ may be enhanced by optimizing the divergence angle of the Bessel photon. Although previous studies suggested that the stellar nucleosynthesis with Bessel photons is different from that with plane wave photons, it is shown that the average cross sections for the Bessel wave and plane wave are identical. This difference between the previous and present studies comes from the integration range of the impact parameter. The previous study (Y. Xu et al. 2024) integrated the transition probability in the limited range, whereas we have integrated it from zero to infinity to obtain the exact result. Even if the Bessel photons are predominately produced in extremely strong magnetic fields, the isotopic abundances of the elements produced in the Universe are not changed.

Acknowledgments

This work was supported by Grants-in-Aid for Scientific Research of JSPS (grant Nos. JP22H01239, JP23K22510, JP24K07057). M.K.C.'s work was supported by the National Research Foundation of Korea (grant Nos. NRF-2020R1A2C3006177 and NRF-2021R1A6A1A03043957). T.K. is supported in part by the National Key R&D Program of China (grant No. 2022YFA1602401) and the National Natural Science Foundation of China (grant No. 12335009 and No. 12435010).

ORCID iDs

Tomoyuki Maruyama https://orcid.org/0000-0002-6691-998X
Takehito Hayakawa https://orcid.org/0000-0001-5286-8395
Myung-Ki Cheoun https://orcid.org/0000-0001-7810-5134
Toshitaka Kajino https://orcid.org/0000-0003-1856-4173

References

Ababekri, M., Guo, R. T., Wan, F., et al. 2024, PhRvD, 109, 016005
Afanasev, A., Carlson, C. E., & Mukherjee, A. 2013, PhRvA, 88, 033841
Afanasev, A., Serbo, V. G., & Solyanik, M. 2018, JPhG, 45, 055102
Afanasev, A., & Carlson, C. E. 2022, AnP, 354, 2100228
Alexandrescu, A., Cojoc, D., & DiFabrizio, E. I. 2006, PhRvL., 96, 243001
Allen, L., Beijersbergen, M. W., Spreeuw, R. J. C., & Woerdman, J. P. 1992, PhRvA, 45, 8185
Anzolin, G., Tamburini, F., Bianchini, A., Umbriaco, G., & Barbieri, C. 2008, A&A, 488, 1159
Babiker, M., Bennett, C. R., Andrews, D. L., & Romero, L. C. D. 2002, PhReL, 89, 143601
Berkhout, G. C. G., & Beijersbergen, M. W. 2008, PhRvL, 101, 100801
Bogdanov, O. V., Kazinski, P. O., & Lazarenko, G. Yu. 2018, PhRvA, 97, 033837
Bogdanov, O. V., Kazinski, P. O., & Lazarenko, G. Yu. 2019, PhRvD, 99, 116016
Chen, Y.-Y., Li, J.-X., Hatsagortsyan, K. Z., & Keitel, C. H. 2018, PhRvL, 121, 074801
de Forest, T., Jr., & Walceck, J. D. 1966, AdPhy, 15, 1
Elias, N. M., II 2008, A&A, 492, 883
Harwit, M. 2003, ApJ, 597, 1266
Hayakawa, T., Iwamoto, N., Shizuma, T., et al. 2004, PhRvL, 93, 161102
Hemsing, E., Knyazik, A., Dunning, M., et al. 2013, NatPh, 9, 549
Jáuregui, R., & Hacyan, S. 2005, PhRvA, 71, 033411
Jentschura, U. D., & Serbo, V. G. 2011, PhRvL, 106, 013001
Katoh, M., Fujimoto, M., Kawaguchi, H., et al. 2017, PhRvL, 118, 094801
Lange, R., Huntemann, N., Peshkov, A. A., Surzhykov, A., & Peik, E. 2022, PhRvL, 129, 253901
Leach, J., Padgett, M. J., Barnett, S. M., Franke-Arnold, S., & Courtial, J. 2002, PhRvL, 88, 257901
Lu, Z. W., Guo, L., Li, Z. Z., et al. 2023, PhRvL., 131, 202502
Mair, A., Vaziri, A., Weihs, G., & Zeilinger, A. 2001, Natur, 412, 313
Markova, M., von Neumann-Cosel, P., & Larsen, A. C. 2021, PhRvL, 127, 182501
Maruyama, T., Hayakawa, T., & Kajino, T. 2019, NatSR, 9, 51
Maruyama, T., Hayakawa, T., Kajino, T., & Cheoun, M.-K. 2022, PhLeB, 826, 136779
Maruyama, T., Hayakawa, Hajima, R. T., Kajino, T., & Cheoun, M.-K. 2023, PhRvR, 5, 043289
McKinney, J. C., Tchekhovskoy, A., & Blandford, R. D, D. 2013, Sci, 39, 49
Mereghetti, S. 2008, A&ARv, 15, 225

Nakamura, K., Kajino, T., Mathews, G. J., Sato, S., & Harikae, S. 2015, A&A, 582, A34
Nishimura, S., et al. 2006, ApJ, 642, 410
Peshkov, A. A., Volotka, A. V., Surzhykov, A., & Fritzsche, S. 2018, PhRvA, 97, 023802
Petrillo, V., Dattoli, G., Drebot, I., & Nguyen, F. 2016, PhRvL, 117, 123903
Picón, A., Benseny, A., Mompart, J., et al. 2010, NJPh, 12, 083053
Portnov, Y. A. 2018, JApA, 39, 38
Sherwin, J. A. 2017, PhRvA, 95, 052101
Schmiegelow, C. T., Schulz, J., Kaufmann, H., et al. 2016, NatCo, 7, 12998
Sieja, K. 2023, EPJA, 59, 147
Shen, Y., Wang, X., Xie, Z., et al. 2019, LSA, 8, 90
Stock, S., Surzhykov, A., Fritzsche, S., & Seipt, D. 2015, PhRvA, 92, 013401
Taira, Y., Hayakawa, T., & Katoh, M. 2017, NatSR, 7, 5018
Tamburini, F., Thidé, B., Molina-Terriza, G., & Anzolin, G. 2011, NatPh, 7, 195
Tamburini, F., Thidé, B., & Valle, M. D. 2020, MNRAS, 492, L22
Utsunomiya, H., Mohr, P., Zilges, A., & Rayet, M. 2006, NuPhA, 777, 459
Woosley, S. E., & Howard, W. M. 1978, ApJS, 36, 285
Xu, Y., Balabanski, D. L., Baran, V., Iorga, C., & Matei, C. 2024, PhLB, 852, 138622
Zhu, X. X., Chen, M., Yu, T.-P., et al. 2018, ApPhL, 112, 174102